JOURNAL OF CHEMICAL EDUCATION

pubs.acs.org/jchemeduc

Demonstration

Water Electrolysis Accompanied by Side Reactions

Kihyang Kim, Seoung-Hey Paik,* and Choong K. Rhee*

Cite This: *J. Chem. Educ.* 2021, 98, 2381−2386

Read Online

ACCESS | Metrics & More | Article Recommendations | Supporting Information

ABSTRACT: Water electrolysis is used to teach important and fundamental concepts in chemistry. In practical water electrolysis experiments, it is difficult to achieve the ideal 2:1 ratio of hydrogen to oxygen. This work demonstrates an experimental setup comprising multiple water electrolysis cells connected in series to simultaneously visualize the effects of various electrode materials and electrolytes on water electrolysis. The volumes of oxygen were lower when using stainless steel and graphite anodes, which corrode in the electrolytes containing SO_4^{2-} and NO_3^- anions, compared to those in the presence of the noncorroding Pt electrode. In addition, the volumes of hydrogen in the presence of NO_3^- anions, which are catalytically reduced on the cathodes of stainless steel and graphite, were remarkably lower than those obtained with the noncatalyzing Pt cathode. These phenomena are attributed to side reactions which consume portions of the electrons intended for water electrolysis. This demonstration can help students to realize that the experimental results of water electrolysis should be carefully interpreted as they may include a contribution from electrode side reactions.

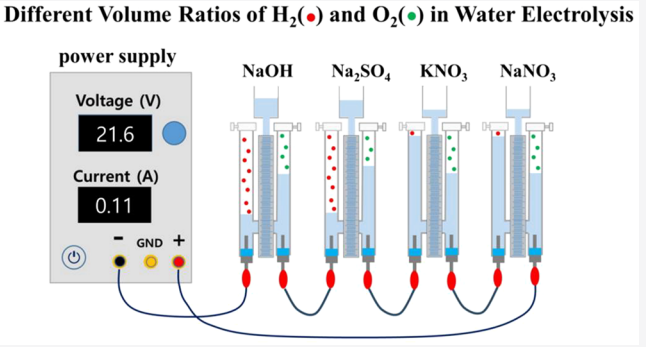

KEYWORDS: *High School/Introductory Chemistry, Demonstrations, Laboratory Instruction, Misconception/Discrepant Events, Oxidation/Reduction, Electrochemistry*

INTRODUCTION

In the course of chemistry education, macroscopic phenomena are understood or taught using pictorial models to understand relevant concepts at the microscopic level.[1] The general way for students to accept a model of interest is to compare the predicted behavior with experimental results:[2,3] If the anticipated behavior is consistent with an observation experienced in the lab or presented in the form of graphs or photographs, then the conceptual model is accepted. One of the most fundamental and conceptually important examples is the electrochemical decomposition of water to hydrogen and oxygen. In fact, most chemistry textbooks[4−6] deal with photographs or schematic drawings of a water electrolysis cell collecting hydrogen and oxygen evolving from the electrodes in an aqueous electrolyte. Furthermore, the pictorial materials emphasize that the volume ratio of hydrogen to oxygen is 2:1.

The importance of water electrolysis in chemical education has led to various studies for the purpose of demonstration in classrooms or laboratories.[7−15] For example, easily available polyethylene pipets and iron wire have been assembled into a Hoffman-like cell to demonstrate water electrolysis.[7] Another example is an assembly of two glass slides sandwiching two pencil lead electrodes, in which the volumes of the evolved gases around the electrodes were measured using photographic image analysis.[8] Although a qualitative demonstration of water electrolysis is easy to perform, a quantitative demonstration of the 2:1 volume ratio is difficult to achieve due to side electrochemical reactions that accompany water electrolysis.

This work presents an experimental setup to demonstrate the influence of side reactions on the volumes of hydrogen and oxygen obtained with water electrolysis. The key point of the experimental setup is the serial connection of a few electrochemical cells consisting of various electrodes and electrolytes, such that the charges flowing through each cell are identical. If the electrodes and the electrolyte in a cell are inert (or not reactive), the volume of the evolved gas will be consistent with the theoretically predicted volume. If not, a deviation will be observed. The experimental setup enables simultaneous comparison of the gas volumes, which enables the recognition of various side reactions depending on the electrode material, polarity, and electrolyte ion. The demonstration using the presented cell configuration will offer an opportunity for students to carefully interpret experimental observations concerning water electrolysis.

Received: January 27, 2021
Revised: May 11, 2021
Published: June 16, 2021

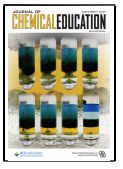

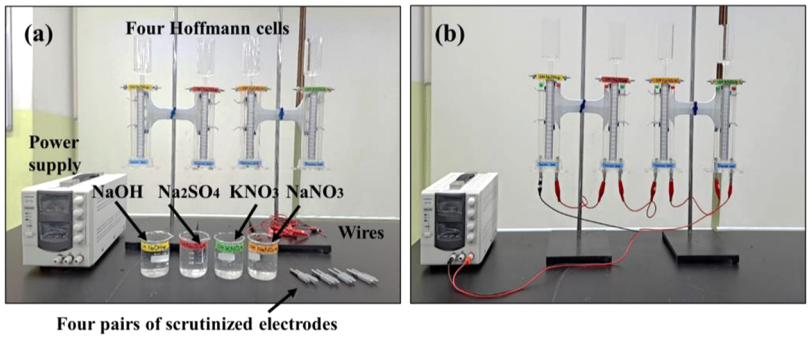

Figure 1. (a) Picture of all the components of an experimental setup and (b) picture of an assembled setup.

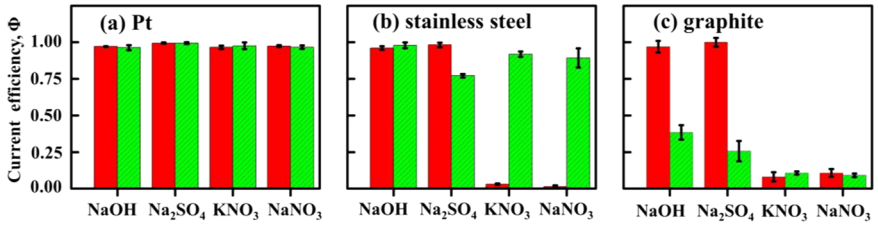

Figure 2. Current efficiencies on the electrodes of (a) Pt, (b) stainless steel, and (c) graphite in water electrolysis. Unhatched and hatched bars correspond to hydrogen and oxygen, respectively. The concentrations of the solutions are 1.0 M. The numerical results are listed in Table S1 in Supporting Information.

EXPERIMENTAL DETAILS

Assembly of Four Cells in Series

Figure 1 presents photographs before and after assembling the experimental setup. All of the components in Figure 1a are detailed in the "Water Electrolysis Experiment" section in the Supporting Information. In Figure 1b, an experimental setup of four Hoffman-type electrolysis cells connected in series is displayed as an example (see video clip 1 in the Supporting Information). A constant current of 0.11 A was allowed to flow through the four cells. The choice of 0.11 A was rather arbitrary; however, the particular current was appropriate to finish the intended demonstration within a reasonable time of ~17 min (see the "Water Electrolysis Experiment" section in the Supporting Information). A current of 0.11 A was maintained by manually adjusting the voltage across the entire circuit from 18 to 22 V. The voltage across each cell ranged from 3 to 10 V, depending on the electrode material and electrolyte.

Materials

The electrode materials were platinized Ti, stainless steel, and graphite. All of the employed electrodes were rod-shaped (length, 70 mm; diameter, 6 mm (graphite, stainless steel) or 3 mm (Pt)), purchased from Mirae Science, Korea. In each Hoffman-type cell, two electrodes of identical materials served as the cathode and anode, respectively. The electrolytes were 1.0 M solutions of NaOH (98%, Samchun Pure Chemical), Na_2SO_4 (99.0%, Daejung Chemicals & Metals), KNO_3 (99.0%, Samchun Pure Chemical), and $NaNO_3$ (99.0%, Daejung Chemicals & Metals).

Definition of Current Efficiency. Current efficiency (Φ) is defined as the ratio of the charge used to evolve a gas (Q_m) to the charge injected into the electrolysis circuit (Q_o), that is, $\Phi = Q_m/Q_o$. In an experiment, Q_m is related to the volume (V_m) of an evolved gas using the following equation. The mole number of the evolved gas is

$$Q_m/n_{gas}F = P_mV_m/RT \quad (1)$$

where F is the Faraday constant, n_{gas} is the mole number of electrons to produce 1 mol of the gas (e.g., n_{gas} = 2 for H_2 ($2H_2O(l) + 2e^- \rightarrow H_2(g) + 2OH^-$); n_{gas} = 4 for O_2 ($2H_2O(l) \rightarrow O_2(g) + 4H^+ + 4e^-$)), R is the gas constant, T is the temperature, and P_m is the pressure of the evolved gas.

Equation 1 can be used to calculate the current efficiency for a gas (Φ) in terms of volume, as follows:

$$\Phi = Q_m/Q_o = \{(n_{gas}F)(P_mV_m/RT)\}/\{(n_{gas}F)(P_oV_o/RT)\} = P_mV_m/P_oV_o \quad (2)$$

where P_o and V_o represent the hypothetical pressure and volume at the temperature of the experiment, respectively, if all the injected charges (Q_o) are used for gas evolution. P_m and P_o would be close enough to each other, if the gas is evolved using all the injected charge and is collected under conditions identical to those of the experiment (see the section "Issues Related to the Main Text" in the Supporting Information). Then, Φ becomes the ratio of the measured volume to the estimated volume, V_m/V_o, as described below:

$$\Phi = Q_m/Q_o = V_m/V_o \quad (3)$$

Furthermore, if the cross-sectional areas of the gas-collecting tubes are the same, V_m and V_o can be expressed in terms of the lengths, L, of the meniscus position changes before and after gas evolution, as follows:

$$\Phi = Q_m/Q_o = V_m/V_o = L_m/L_o \quad (4)$$

Therefore, L is equivalent to the volume of the evolved gas, such that the current efficiency values are calculable with the meniscus position changes.

When Φ is equal to 1, all the injected electrons are consumed in evolving hydrogen or oxygen; when Φ is less than 1, some side reactions consume a portion of the injected electrons. The content of the side reactions is obviously (1 −

https://doi.org/10.1021/acs.jchemed.1c00072
J. Chem. Educ. 2021, 98, 2381−2386

Φ). When Φ values for both hydrogen and oxygen are 1, the volume ratio of hydrogen and oxygen is 2:1.

The current efficiencies presented in this work are the averaged values of more than three replicated experimental results.

EXPLANATION OF EXPERIMENTAL RESULTS

Current Efficiencies of Real Water Electrolysis

Figure 2 shows the current efficiencies of hydrogen and oxygen from the electrodes of Pt, stainless steel, and graphite in 1.0 M solutions of NaOH, Na_2SO_4, KNO_3, and $NaNO_3$. With Pt electrodes, the Φ values of hydrogen and oxygen were close 1, regardless of the electrolyte (Figure 2a). The hydrogen current efficiencies obtained with the stainless steel cathodes were close to 1 in the solutions of NaOH and Na_2SO_4, while those in the solutions of KNO_3 and $NaNO_3$ remarkably decreased close to 0 (Figure 2b). However, the oxygen current efficiencies of stainless steel anodes were in the range 0.8−0.9 for all electrolytes, except for the NaOH solution. For the graphite electrodes, Figure 2c shows that, for all the scrutinized solutions, the Φ values for oxygen were below 0.5, whereas those for hydrogen were ∼1 only in the solutions of NaOH and Na_2SO_4. Thus, the current efficiencies of hydrogen and oxygen clearly depend on the electrode material, electrode polarity, and electrolyte.

Reason for the Low Current Efficiency of Oxygen Evolution

The side reaction that diminishes the current efficiency for oxygen evolution at the anodes is related to the oxidation (or corrosion) of the electrode itself. The current efficiency for oxygen evolution with graphite anodes is quite low, indicating that oxidation reactions other than oxygen evolution take place extensively. Graphite is known to corrode in electrochemical environments.[16−22] Specifically, carbon atoms at the edges and defect sites of graphene layers stacked in graphite have been reported to readily oxidize in anodic electrochemical environments to various oxygen-containing surface carbon functional groups, such as carboxylic acids and aldehydes[17−19] (e.g., graphitic C → graphitic C−X; X = OH, O, COOH, etc.) and even to gaseous CO or CO_2 (e.g., graphitic C + H_2O → $CO(g) + 2H^+ + 2e^-$ or graphitic C + $2H_2O$ → $CO_2(g) + 4H^+ + 4e^-$).[20−22] Furthermore, the evolution of oxygen gas within graphene layers bursts the layers, causing exfoliation.[19,22−26] Moreover, the exfoliated graphene edges further accelerate the formation of oxygenated surface carbons. As shown in Figure 3a, the color and porosity of the graphite anode changed after severe corrosion. Therefore, the graphite anode consumes most of the injected electrons in the process of corrosion.

Stainless steel is also somewhat inefficient for oxygen formation, as the Φ value for oxygen evolution is in the range 0.8−0.9 in all electrolyte solutions except for the NaOH solution (Figure 2b). An electrochemical reaction of metallic species, such as Fe and Cr, in stainless steel to soluble species (i.e., corrosion reactions such as $M(s) \rightarrow M^{n+}(aq) + ne^-$, M = Fe, Mn, Cr, Ni, etc.)[27−30] would be responsible for the small decrease in the current efficiency for oxygen evolution. In fact, the shiny surface of the stainless steel changed after oxygen evolution, as shown in Figure 3b. In contrast, the stainless steel anode in the NaOH electrolyte did not lose its shine, indicating that stainless steel did not corrode, maintaining a current efficiency of ∼1. Furthermore, the higher current efficiency of stainless steel compared to that of graphite implies that the corrosion of stainless steel was much slower, allowing oxygen evolution to consume a greater portion of the injected electrons.

In the case of the Pt anode, the Φ values for oxygen are close to the ideal value of 1 regardless of the electrolyte, indicating that no corrosion took place on inert Pt.

Reason for the Low Current Efficiency of Hydrogen Evolution

The current efficiency of hydrogen evolution at the cathode depends on the type of anion in the electrolyte and the electrode. As demonstrated in Figure 2, the Φ values for hydrogen are ∼1 in the presence of OH^- and SO_4^{2-} anions, regardless of the electrode material, implying that the particular anions were inert with respect the cathodes of the studied materials. However, in the presence of NO_3^- anions, the Φ values obtained with stainless steel and graphite cathodes are quite low, but that of the Pt cathode is not. NO_3^- anions are known to be electrochemically reduced to other N-containing species such as NO_2^- and NH_2OH (e.g., $NO_3^- + H_2O + 2e^- \rightarrow NO_2^- + 2OH^-$, $NO_2^- + 4H_2O + 4e^- \rightarrow NH_2OH + 5OH^-$).[17,20,21,31−33] However, Figure 2 clearly indicates that only the surfaces of stainless steel and graphite catalyzed the reduction of NO_3^- anions to consume most of the injected electrons. Figure 4 shows the dependence of the Φ value for hydrogen evolution on the concentration of NO_3^- anions with stainless steel. Specifically, the Φ value for hydrogen evolution with stainless steel increases from 0.03 to 0.30 as the concentration of the NO_3^- anion decreases from 1.0 to 0.1 M, suggesting that more injected electrons are consumed in the NO_3^- reduction as more NO_3^- anions are available to the electrode. In addition, the slightly higher Φ values obtained with graphite compared to those with stainless steel indicate that the latter catalyzes NO_3^- reduction more effectively than the former. Likewise, the Φ value of 1 with the Pt cathode verifies that there is no catalytic reduction of NO_3^- anions or that NO_3^- anions are inert with respect to Pt. It should be

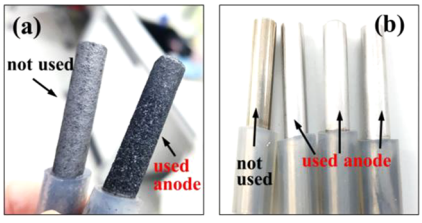

Figure 3. Photographs of (a) graphite and (a) stainless steel anodes before and after oxygen evolution.

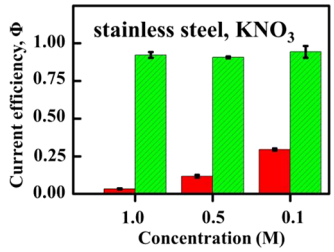

Figure 4. Current efficiencies on stainless steel electrode in the KNO_3 solutions of different concentrations. Unhatched and hatched bars correspond to hydrogen and oxygen, respectively.

https://doi.org/10.1021/acs.jchemed.1c00072
J. Chem. Educ. 2021, 98, 2381−2386

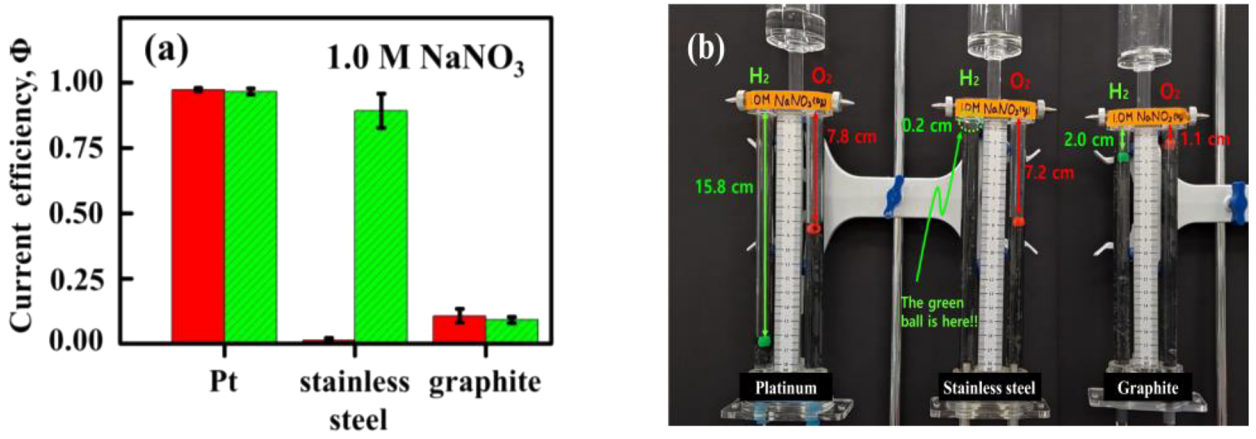

Figure 5. Relations between current efficiency and volume ratio. (a) The current efficiencies of hydrogen and oxygen on platinum, stainless steel, and graphite, extracted from Figure 2. (b) The evolved volumes of hydrogen and oxygen in 1.0 M $NaNO_3$ solution. The green and red balls in the columns indicate the solution levels. The volume of an evolved gas is equivalent to the change of meniscus position before and after an experiment, expressed with the double-headed arrow.

noted that the K^+ and Na^+ cations did not affect the reduction of NO_3^- anions.

Current Efficiency versus the Volume Ratio of Hydrogen to Oxygen

Figure 5 demonstrates the correlation between the current efficiency and the volume ratio of hydrogen to oxygen evolved in a 1.0 M $NaNO_3$ solution. With Pt electrodes, both of the current efficiencies are ~1, and the volume ratio (actually the ratio of the column lengths for hydrogen and oxygen) is 2:1 or 2. In the case of stainless steel, the apparent volume ratio is ~0:1 or 0, due to the preferential reduction of NO_3^- anions such that hydrogen does not evolve. The volume ratio in the graphite cell is close to 2:1 or 1.8. It should be recalled that the current efficiencies for the gases with graphite are far below 1, as revealed by the much lower absolute amounts of the gases compared with those obtained with Pt. The reason for the particular volume ratio on graphite (1.8) is that the current efficiencies for both gases are similar. Therefore, it is important to recognize the side reactions or side reactions involved in each electrode during water electrolysis.

Ideal Cell versus Real Cell

In an electrolytic cell in which actual electrolytic reactions of oxidation and reduction take place to flow a current, the roles of the electrodes and electrolyte need to be clarified. In an ideal cell, the electrode is an inert interface for electrons to transfer between an external circuit and the reactants of interest in solution, and the electrolyte is an inert ionic conductor for the charge to flow between the two electrodes. However, the electrodes and electrolyte in a real cell do not frequently follow the ideal behavior, as demonstrated in this work. If they are reactive, the injected electrons will divert from the intended reactions to side reactions (e.g., corrosion of the electrode and reduction of NO_3^- ions). Thus, attention should be paid to interpreting observations during water electrolysis driven by a current flow.

Why Is Water Electrolysis Accompanied by Side Reactions?

Figure 6 presents hypothetical potential−current (polarization) curves of water electrolysis and the accompanying side reactions. The onset potential and slope of an electrochemically active species certainly depend on electrode material and electrolyte composition containing the reactant.

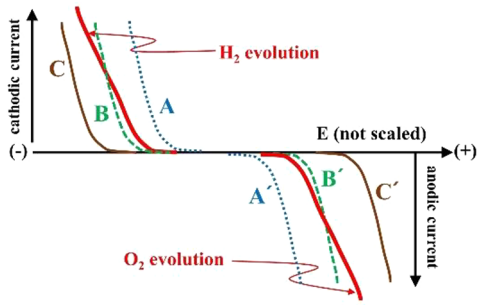

Figure 6. Hypothetical potential−current (polarization) curves of water electrolysis and accompanying side reactions.

Therefore, actual polarization curves are obtainable only with experiments (which are certainly beyond the scope of this work) but not calculable with the thermodynamic Nernst equation. However, the hypothetical curves in Figure 6 would be good enough to explain the observations in this work for an education purpose.

A constant current flow through an electrochemical cell needs certain electrolytic oxidative and reductive reactions simultaneously occurring on the respective anode and cathode to accommodate the given current. If a number of reactions on an electrode are available, the promptest one takes place to allow the forced current flow. The promptness of a reaction is reflected by the onset potential (or overpotential) in the polarization curve. For instance, if H_2 evolution and cathodic side reaction A can take place, side reaction A will preferentially consume most of the injected electrons, because side reaction A needs less potential energy (or a smaller overpotential) for the requested current flow. Indeed, NO_3^- reduction on the cathodes of stainless steel and graphite is the case of side reaction A. When side reaction B is available, H_2 evolution and side reaction B take place at the same time so that the amount of H_2 will be significant but less than the theoretical one (not observed in this work). In the case of side reaction C, only H_2 evolution will take place, as observed with Pt in all of the studied solutions, and with stainless steel and graphite in the solutions of OH^- and SO_4^{2-}. Such a difference in the position of polarization curve for an electrochemical reaction is that electrode material and electrolyte composition determine the reaction rate (or equivalently the overpotential)

https://doi.org/10.1021/acs.jchemed.1c00072
J. Chem. Educ. 2021, 98, 2381−2386

of an electroactive species of interest. In other words, stainless steel and graphite catalyzed only NO_3^- reduction under the employed condition in this work, while Pt did not.

The variation in the amount of evolved O_2 can be understood from the identical point of view. Graphite corrosion corresponds to side reaction A′ because O_2 evolution was overwhelmed. Side reaction B′ is consistent with stainless steel corrosion due to the significant amount of generated O_2. No side reaction was observed on Pt anode in the studied solutions, so that the polarization curve of a side reaction on Pt (if any) would be that of side reaction C′.

One may raise a question on a possible oxidation reaction of SO_4^{2-} to $S_2O_8^{2-}$ (an excellent oxidizing agent). Because the standard reduction potential of $S_2O_8^{2-}$ to SO_4^{2-} (+2.01 V) is much higher than that of H_2O to O_2 (+1.229 V),[34] it is easily predictable from thermodynamics that $S_2O_8^{2-}$ production is much harder than O_2 evolution. For successful electrochemical formation of $S_2O_8^{2-}$, the polarization curve of O_2 evolution should be shifted in the positive potential direction beyond that of oxidation of SO_4^{2-} to $S_2O_8^{2-}$, meaning that an anode with an extremely high overpotential for O_2 evolution is absolutely demanded. Such a high overpotential of O_2 evolution was achieved on a B-doped diamond anode in highly concentrated H_2SO_4 solution.[35] In fact, the positive working potential limit of B-doped diamond in 1 M H_2SO_4 solution is +1.7 V (even that of fluorinated B-doped diamond is +2.5 V), while that of Pt is 0.9 V.[36] Thus, the polarization curve of SO_4^{2-} oxidation would be that of side reaction B′ on B-doped diamond, while it would be that of side reaction C′ on Pt.

DEMONSTRATIONS

A three-step activity is recommended, as detailed in the section titled "Guideline for Teachers" in the Supporting Information. Briefly, the first step is an introductory activity for students to summarize the knowledge regarding water electrolysis by completing a predemo report with a handout. The next is a demonstration step, in which a teacher can use video clips 1−3 provided in the Supporting Information, or a teacher can carry out the experiments suggested in the section "Water Electrolysis Experiment" in the Supporting Information. The last step is a closing activity to draw a conclusion with an analysis of the observations and to answer the questions in the postdemo report. In the case of a demonstration using video clips, the numerical results given at the ends of video clips 2 and 3 can be utilized, and in the case of a demonstration, the numerical results should be obtained from the actual experiments. In both cases, the data sheet in the Supporting Information should be completed before answering the questions in the postdemo report in the Supporting Information. The teacher can hold a discussion with the students based on the predemo report, data sheet, and postdemo report.

HAZARDS

Sodium hydroxide can be dangerous (corrosive, causing severe chemical burns and blindness upon contact with the eyes). KNO_3, $NaNO_3$, and Na_2SO_4 can cause irritation to the skin, eyes, and respiratory tract and may be harmful if swallowed or inhaled. Thus, protective equipment, such as rubber gloves, safety clothing, and eye protection, should always be used when handling this chemical or its solutions. After electrolysis, the nitrate solution became basic in this study. Therefore, the KNO_3 and $NaNO_3$ solutions should be discarded.

CONCLUSIONS

An electrochemical system of multiple cells in series was demonstrated to simultaneously visualize the influences of different electrode materials and electrolytes on water electrolysis under a constant current flow. The particular experimental setup provides a demonstration of the basic concepts of electrolysis, such as the roles of electrodes and electrolytes, Faraday's law, and the current efficiency related to side reactions. In particular, the strict experimental requirements for observation of the ideal volume ratio of hydrogen to oxygen (2:1) in water electrolysis (as one of the most popular and fundamental models in chemistry education) suggest that any underlying assumptions associated with conceptual models (e.g., inert electrodes and electrolytes in water electrolysis) should be clearly understood. With this demonstration, students can learn that interpretation of the observed results from water electrolysis needs to take into account the nonideality of the process by inclusion of the accompanying side reactions.

ASSOCIATED CONTENT

Supporting Information

The Supporting Information is available at https://pubs.acs.org/doi/10.1021/acs.jchemed.1c00072.

Issues related to the main text, guidelines for the teacher, water electrolysis experiment, hazards, handouts for the students, predemo report, data sheet, postdemo report, and description of the videos (PDF, DOCX)

Video clip 1 showing how to install an experimental apparatus, how to connect circuits, and how to adjust the voltage to pass a constant current during the experiment (AVI)

Video clip 2 demonstrating water electrolysis in the 1.0 M $NaNO_3$ solution using Pt, stainless steel, and graphite electrodes with a current of 0.11 A for 16 min (AVI)

Video clip 3 demonstrating water electrolysis in the 1.0 M solutions of NaOH, Na_2SO_4, $NaNO_3$, and KNO_3 using stainless steel electrodes with a current of 0.11 A for 16 min (AVI)

AUTHOR INFORMATION

Corresponding Authors

Choong K. Rhee − *Department of Chemistry, Chungnam National University, Daejeon 34134, Republic of Korea;* orcid.org/0000-0002-4442-6164; Email: ckrhee@cnu.ac.kr

Seoung-Hey Paik − *Department of Chemistry Education, Korea National University of Education, Cheongju City 28173, Republic of Korea;* orcid.org/0000-0002-3822-3838; Email: shpaik@knue.ac.kr

Author

Kihyang Kim − *Department of Chemistry Education, Korea National University of Education, Cheongju City 28173, Republic of Korea;* orcid.org/0000-0001-9712-5958

Complete contact information is available at: https://pubs.acs.org/10.1021/acs.jchemed.1c00072

https://doi.org/10.1021/acs.jchemed.1c00072
J. Chem. Educ. 2021, 98, 2381−2386

Notes

The authors declare no competing financial interest.

REFERENCES

(1) *Multiple Representations in Chemical Education*; Gilbert, J. K., Treagust, D. F., Eds.; Springer: New York, 2009; Vol. *4*, pp 1−8.
(2) Giere, R. N. A new framework for teaching scientific reasoning. *Argumentation* **2001**, *15* (1), 21−33.
(3) Justi, R.; Gilbert, J. Models and Modelling in Chemical Education. In *Chemical Education: Towards Research-Based Practice*; Springer: Dordrecht, 2002; pp 47−68.
(4) Chang, R.; Overby, J. *General Chemistry: The Essential Concepts*, 3rd ed.; McGraw-Hill: New York, 2000; pp 843−850.
(5) Oxtoby, D.; Gillis, H.; Butler, L. *Principles of Modern Chemistry*, 8th ed.; Cengage Learning: Boston, MA, 2016; pp 3−6.
(6) Zumdahl, S. S.; Zumdahl, S. A. *Chemistry*, 8th, International Student, ed.; Cengage Learning: Boston, MA, 2010; pp 847−852.
(7) Eggen, P. O.; Kvittingen, L. A small-scale and low-cost apparatus for the electrolysis of water. *J. Chem. Educ.* **2004**, *81* (9), 1337.
(8) Ling, Y.; Chen, P.; Li, J.; Zhang, J.; Chen, K. Using Image Recognition and Processing Technology to Measure the Gas Volume in a Miniature Water Electrolysis Device Constructed with Simple Materials. *J. Chem. Educ.* **2020**, *97* (3), 695−702.
(9) Suzuki, C. A new low-cost apparatus for electrolysis of water. *J. Chem. Educ.* **1995**, *72* (10), 912.
(10) Davis, T. A.; Athey, S. L.; Vandevender, M. L.; Crihfield, C. L.; Kolanko, C. C. E.; Shao, S.; Ellington, M. C. G.; Dicks, J. K.; Carver, J. S.; Holland, L. A. Electrolysis of water in the secondary school science laboratory with inexpensive microfluidics. *J. Chem. Educ.* **2015**, *92* (1), 116−119.
(11) Kamata, M.; Yajima, S. Microscale electrolysis using coin-type lithium batteries and filter paper. *J. Chem. Educ.* **2013**, *90* (2), 228−231.
(12) Hendel, S. J.; Young, E. R. Introduction to electrochemistry and the use of electrochemistry to synthesize and evaluate catalysts for water oxidation and reduction. *J. Chem. Educ.* **2016**, *93* (11), 1951−1956.
(13) Dabke, R. B.; Gebeyehu, Z. Using mole ratios of electrolytic products of water for analysis of household vinegar: an experiment for the undergraduate physical chemistry laboratory. *J. Chem. Educ.* **2012**, *89* (9), 1198−1200.
(14) Hoffman, B.; Mitchell, E.; Roulhac, P.; Thomes, M.; Stumpo, V. M. Determination of the fundamental electronic charge via the electrolysis of water. *J. Chem. Educ.* **2000**, *77* (1), 95.
(15) Stowe, R. L.; Bischof, S. M.; Konnick, M. M.; Hövelmann, C. H.; Leach-Scampavia, D.; Periana, R. A.; Hashiguchi, B. G. Making Water the Exciting Way: A Classroom Demonstration of Catalysis. *J. Chem. Educ.* **2014**, *91* (4), 550−553.
(16) Tsuji, R.; Masutani, H.; Haruyama, Y.; Niibe, M.; Suzuki, S.; Honda, S.-i.; Matsuo, Y.; Heya, A.; Matsuo, N.; Ito, S. Water Electrolysis using Flame-Annealed Pencil-Graphite Rods. *ACS Sustainable Chem. Eng.* **2019**, *7* (6), 5681−5689.
(17) Zhang, G.; Wen, M.; Wang, S.; Chen, J.; Wang, J. Insights into electrochemical behavior and anodic oxidation processing of graphite matrix in aqueous solutions of sodium nitrate. *J. Appl. Electrochem.* **2016**, *46* (12), 1163−1176.
(18) Rueffer, M.; Bejan, D.; Bunce, N. J. Graphite: An active or an inactive anode? *Electrochim. Acta* **2011**, *56* (5), 2246−2253.
(19) Besenhard, J. O.; Fritz, H. P. The electrochemistry of black carbons. *Angew. Chem., Int. Ed. Engl.* **1983**, *22* (12), 950−975.
(20) Dadang, S.; Kawanishi, T.; Shimizu, N.; Hayashi, Y. Nitrate removal rate in a continuous column denitrification reactor using hydrogen generated by electrolysis with carbon anodes and stainless cathodes. *Water Sci. Technol.* **2002**, *46* (11−12), 39−44.
(21) Sakakibara, Y.; Araki, K.; Watanabe, T.; Kuroda, M. The denitrification and neutralization performance of an electrochemically activated biofilm reactor used to treat nitrate-contaminated groundwater. *Water Sci. Technol.* **1997**, *36*, 61−68.
(22) Goss, C. A.; Brumfield, J. C.; Irene, E. A.; Murray, R. W. Imaging the incipient electrochemical oxidation of highly oriented pyrolytic graphite. *Anal. Chem.* **1993**, *65* (10), 1378−1389.
(23) Abdelkader, A. M.; Cooper, A. J.; Dryfe, R. A. W.; Kinloch, I. A. How to get between the sheets: a review of recent works on the electrochemical exfoliation of graphene materials from bulk graphite. *Nanoscale* **2015**, *7* (16), 6944−6956.
(24) Parvez, K.; Wu, Z. S.; Li, R.; Liu, X.; Graf, R.; Feng, X.; Mullen, K. Exfoliation of graphite into graphene in aqueous solutions of inorganic salts. *J. Am. Chem. Soc.* **2014**, *136* (16), 6083−6091.
(25) Freund, M. S.; Brajter-Toth, A.; Cotton, T. M.; Henderson, E. R. Scanning tunneling microscopy and atomic force microscopy in the characterization of activated graphite electrodes. *Anal. Chem.* **1991**, *63* (10), 1047−1049.
(26) Alsmeyer, D. C.; McCreery, R. L. In situ Raman monitoring of electrochemical graphite intercalation and lattice damage in mild aqueous acids. *Anal. Chem.* **1992**, *64* (14), 1528−1533.
(27) Li, L. F.; Caenen, P.; Jiang, M. F. Electrolytic pickling of the oxide layer on hot-rolled 304 stainless steel in sodium sulphate. *Corros. Sci.* **2008**, *50* (10), 2824−2830.
(28) Wendt, J. L.; Chin, D. T. The ac corrosion of stainless steel—II. The polarization of ss304 and ss316 in acid sulfate solutions. *Corros. Sci.* **1985**, *25* (10), 901−915.
(29) Hildén, J. M. K.; Virtanen, J. V. A.; Ruoppa, R. L. K. Mechanism of electrolytic pickling of stainless steels in a neutral sodium sulphate solution. *Mater. Corros.* **2000**, *51* (10), 728−739.
(30) Kovendhan, M.; Kang, H.; Jeong, S.; Youn, J. S.; Oh, I.; Park, Y. K.; Jeon, K. J. Study of stainless steel electrodes after electrochemical analysis in sea water condition. *Environ. Res.* **2019**, *173*, 549−555.
(31) Ding, J.; Li, W.; Zhao, Q. L.; Wang, K.; Zheng, Z.; Gao, Y. Z. Electroreduction of nitrate in water: Role of cathode and cell configuration. *Chem. Eng. J.* **2015**, *271*, 252−259.
(32) Katsounaros, I.; Kyriacou, G. Influence of nitrate concentration on its electrochemical reduction on tin cathode: Identification of reaction intermediates. *Electrochim. Acta* **2008**, *53* (17), 5477−5484.
(33) Garcia-Segura, S.; Lanzarini-Lopes, M.; Hristovski, K.; Westerhoff, P. Electrocatalytic reduction of nitrate: Fundamentals to full-scale water treatment applications. *Appl. Catal., B* **2018**, *236*, 546−568.
(34) Skoog, D. A.; Holler, F. J.; Crouch, S. R. *Principles of Instrumental Analysis*; Cengage Learning, 2017; pp 915−916.
(35) Hippauf, F.; Dörfler, S.; Zedlitz, R.; Vater, A.; Kaskel, S. Continuous electrooxdiation of sulfuric acid on boron-doped diamond electrodes. *Electrochim. Acta* **2014**, *147*, 589−595.
(36) Harris, D. C. *Quantitative Chemical Analysis*; W.H. Freeman: New York, 2010; p 377.

https://doi.org/10.1021/acs.jchemed.1c00072
J. Chem. Educ. 2021, 98, 2381−2386